Article

Effect of Annealing on the Magnetic Properties of Co$_2$MnSi-Based Heusler Alloy Glass-Coated Microwires

Mohamed Salaheldeen [1,2,3,4,*] , Mihail Ipatov [1,2,4] , Paula Corte-Leon [1,2,4] , Valentina Zhukova [1,2,4] and Arcady Zhukov [1,2,4,5,*]

1 Departamento de Polímeros y Materiales Avanzados, Facultad Química, Universidad del País Vasco, UPV/EHU, 20018 San Sebastián, Spain
2 Departamento de Física Aplicada, EIG, Universidad del País Vasco, UPV/EHU, 20018 San Sebastián, Spain
3 Physics Department, Faculty of Science, Sohag University, Sohag 82524, Egypt
4 EHU Quantum Center, University of the Basque Country, UPV/EHU, 20018 San Sebastián, Spain
5 IKERBASQUE, Basque Foundation for Science, 48011 Bilbao, Spain
* Correspondence: mohamed.salaheldeenmohamed@ehu.eus (M.S.); arkadi.joukov@ehu.eus (A.Z.)

Abstract: In the current study, we concentrated on the influence of annealing on the magnetic behavior of Co$_2$MnSi-based Heusler microwires. We set the annealing temperature at 1023 K for 2 h, as the sample did not show any significant changes in the magnetic properties at lower temperatures, while annealing at temperatures above 1023 K damages the glass coating. Strong in-plane magnetocrystalline anisotropy parallel to the microwire axis was evident in the magnetic behavior at room temperature for as-prepared and annealed samples. The coercivity of the annealed sample was four times higher than that of the as-prepared sample across a wide range of measuring temperatures. Both annealed and as-prepared samples exhibit quite stable coercivity behavior with temperature, which may have interesting applications. The annealed sample did not exhibit magnetic saturation for M-H loops measured below 50 K. Sharp irreversible magnetic behavior has been detected for annealed samples at a blocking temperature of 220 K; at the same time, the blocking temperature for the as-prepared sample was 150 K. The strong internal mechanical stress induced during the fabrication of Co$_2$MnSi microwires in addition to the internal stress relaxation caused by the annealing induced the onset of magnetic phases resulting in unusual and irreversible magnetic behavior.

Keywords: Heusler alloys; glass-coated microwires; magnetic properties; annealing; blocking temperature

1. Introduction

Amorphous and nanocrystalline glass-coated micro- and nanowires are particularly intriguing materials in terms of both theory and technological applications. Taylor developed a straightforward manufacturing process for casting short samples of glass-coated micro- and nanowires in 1924 [1]. This method was later (between 1950 and 1964) extensively modified by Ulitovsky, who provided a receiving bobbin, which enabled the preparation of quite long (almost continuous) glass-coated microwires [2]. Large quantities of these microwires may be produced using the modified Taylor–Ulitovsky process [3]. Additionally, the modern fabrication facility for glass-coated microwire preparation is provided with a feedback system that allows for precise control of the microwire geometry (metallic nucleus diameter, d, and the total of all microwire diameters, D) using a PC [4]. Accordingly, studies of glass-coated microwires have attracted substantial interest in recent years, largely due to their technical uses, particularly as sensor components in various systems [5]. Microwires play a significant role in a variety of applications, the majority of which are connected to wireless telecommunications systems, such as satellite global positioning, broadcast satellite television, and cellular telephones as well as various magnetic sensors. Radar systems are also particularly helpful for a number of remote sensing systems, including air traffic control radar, missile tracking radar, and sea radar for identifying moving targets [3–5].

Ferromagnetic-based, glass-coated microwires are among the most promising functional magnetic materials, because of their unique combination of physical (mechanical, magnetic, and anticorrosive) qualities and their fast, low-cost preparation method [3,6].

Among the promising ferromagnetic alloys are Heusler alloys, which have compositions of X_2YZ (full-Heusler) or XYZ (half-Heusler), where X and Y are transition metals and Z is the major group element; these belong to a category of materials having several applications [7]. Due to the presence of a band gap around the Fermi energy, the majority of the spin bands in this class of materials exhibit metallic behavior, while the minority of the spin bands exhibit semiconducting or insulating features [8–10]. Therefore, at the Fermi level, these materials exhibit nearly 100% spin polarization [11].

Due to their high Curie point (Tc > 1200 K), adjustable band structure, and low magnetic damping coefficients, Co-based Heusler compounds are among the most promising materials for multifunctional applications [12–14]. Because of the significant Berry curvature associated with their band structure, these alloys also exhibit remarkable and anomalous physical characteristics above and below room temperature [15,16]. As a result, Co-based Heusler compounds are gaining the interest of the scientific community, and extensive studies and investigations have been carried out. Co_2MnSi is a strong option for an advanced spintronic device, because of its high band gap for minority spins (0.5 to 0.8 eV), high Curie temperature (985 K), high tunnel magnetoresistance, large magnetoresistance ratios, and perpendicular magnetic anisotropy [17–20]. In the last two decades, both experimental and theoretical research on Co_2MnSi have concentrated on the examination of its structural and magnetic characteristics and on their relationship to spin polarization [21–23]. By using ultraviolet-photoemission spectroscopy, the maximum value of spin polarization for bulk Co_2MnSi (93%) was found at room temperature [24]. The properties mentioned above make the Co_2MnSi Heusler alloy one of the most investigated Co-based Heusler compounds and a suitable material for spintronic applications.

Arc melting is the most widely used method for fabricating the magnetic Heusler alloy, followed by thermal treatment to enhance its physical structure [25,26]. Using this technique, it was possible to create large-scale Heusler alloys with adjustable chemical compositions. Additionally, according to reports elsewhere [26,27], several processes are used to produce Heusler alloys in a variety of forms, including thin films, nanoparticles, ribbons, and nanostructured materials. As previously mentioned, miniaturization allows for the modification and enhancement of several physical features of bulk Heusler alloys [26,28–31].

However, there are a number of issues and difficulties with the preparation of any prospective "multifunction and smart" Heusler alloy. The first involves large-scale production of alloys made from Heusler compounds that have the exact same chemical make-up and physical characteristics. In addition, specialized processes are expensive and demand extremely precise physical requirements (ultra-high vacuum, pressure, power, high temperature, and a specific substrate). Modern Taylor–Ulitovsky fabrication facilities make it possible to fabricate ultra-thin and uniform glass-covered microwires, a composite material consisting of a metallic nucleus (diameter 0.1–100 μm) covered by a glass coating (thickness 2–30 μm) [3,32]. It is a very promising approach for the creation of multifunctional, smart materials for a wide variety of applications, due to the low cost of large-scale manufacturing (i.e., many kilometers from a tiny ingot (5 g)). Furthermore, the versatility of creating Heusler-based, glass-coated microwires with various structures, including amorphous, nanocrystalline, and granular, offers a special opportunity to study the impact of various microstructure types of the same material on its physical properties [32–38]. Additionally, a flexible, insulating, continuous glass coating offers electrical short-circuit protection, enabling the usage of Heusler-based, glass-coated microwires in environments with harsh chemicals, as well as offering biocompatibility for Heusler alloys' often biologically incompatible structure [39–41]. However, to the best of our knowledge, such promising Heusler alloys, i.e., Co_2MnSi-based, glass-coated microwires, have not been investigated before. Therefore, we consider this study, along with our previous study [42], to be pioneering

investigations aimed at revealing the main magneto-structural properties of Co_2MnSi glass-coated microwires. Some magnetic and structural properties, such coercivity, temperature stability, and irreversibility behavior have not been found in Co_2MnSi in other physical forms, such as thin films [17–23]. An important point for these differences is the unique internal mechanical stress distribution, which is induced during the fabrication process and determines the magneto-structural behavior. This kind of internal stress distribution can be easily controlled during the fabrication process. In our previous study, we illustrated the magneto-structural properties of as-prepared Co_2MnSi glass-coated microwires [42]. In the current study, we focused on the effect of thermal annealing on the magnetic properties of Co_2MnSi glass-coated microwires. We found that annealing greatly effects magnetic behavior. In addition, we found stable magnetic and structural behavior for annealing temperatures below T = 1023 K.

2. Materials and Methods

The facile evaporation of Mn, which would affect the actual nominal composition ratio, made it difficult to fabricate Co_2MnSi glass-coated microwires with a ratio of (2:1:1), i.e., $Co_{50}Mn_{25}Si_{25}$. As a result, we began by employing a traditional arc furnace and additional Mn mass to make the Co_2MnSi alloy. To prevent the Co_2MnSi alloy from oxidizing during the melting process, we melted high-purity metals Co (99.99%), Si (99.99%), and Mn (99.99%) supplied by Technoamorf S.R.L. Co. (Turku, Finland) under vacuum and in an argon environment. Five melting cycles were required to produce a uniform, highly homogenous Co_2MnSi alloy. Afterwards, we used Scanning Electron Microscopy (SEM) and Energy Dispersive X-ray (EDX) (JEOL-6610LV, JEOL Ltd., Tokyo, Japan) to determine the nominal chemical composition of the Co_2MnSi alloy. Once we had the correct alloy composition, we began the manufacture of Co_2MnSi glass-coated microwires using the Taylor–Ulitovsky approach after confirming the nominal ratio of (2(Co):1(Mn):1(Si)), which entailed drawing and casting straight from the melted $Co_{50}Mn_{25}Si_{25}$ alloy as detailed elsewhere [42–44]. A glass capillary was formed after a high frequency inductor heated an ingot over its melting point. This glass capillary was then filled with the molten Co_2MnSi alloy, pulled out, and wrapped onto a revolving pick-up bobbin [3,43,45]. The diameter of the metallic nuclei, d, was governed by the speed of wire drawing and the speed of the pick-up bobbin rotation. Additionally, passing the produced microwire through a coolant stream resulted in rapid melt quenching [43,46]. We evaluated the geometric characteristics of Co_2MnSi glass-coated microwires using SEM, where the metallic nucleus diameter of the Co_2MnSi produced microwire was d_{nuclei} = 10.2 $\pm$ 0.1 μm and the overall diameter D_{total} = 22.2 $\pm$ 0.1 μm. The most intriguing aspect of the manufacturing method is that, during the rapid solidification process, the metallic nuclei were surrounded by a glass layer, protecting them from oxidation and making this the perfect procedure for Mn-based alloys. Additionally, such a process is linked to elevated internal stresses brought on by rapid quenching itself, by drawing stresses, and by the internal stress originating from the different thermal expansion coefficients of the glass and the metallic nuclei [5,44,47–50]. After preparation of the Co_2MnSi glass-coated microwires, annealing was performed at 1023 K for two hours in a conventional furnace in an air atmosphere (insulating glass-coating offers excellent oxidation protection). At an annealing temperature, T_{ann}, above 1023 K and an annealing time above 2 h at T_{ann} = 1023 K, the glass-coating of Co_2MnSi glass-coated microwire begins to be damaged and, at a higher T_{ann}, can completely disappear. Thus, we only focused on the annealing conditions where glass-coated microwires were not yet damaged. As previously reported, annealing conditions (T_{ann}, and time annealing, t_{ann}) and even cooling conditions after annealing are important. Therefore, in this case, to reduce disorder and internal stresses, we applied slow (with a furnace) cooling [43]. Next, the chemical compositions of the samples were determined by EDX. The average chemical composition of around $Co_{51}Mn_{23.9}Si_{25.1}$ proved the validity of the nominal ratio (2:1:1), and the real chemical composition was determined by analyzing the different 10 points as detailed in our earlier study [42]. Recently, X-ray Diffraction (XRD) BRUKER (D8 Advance,

Bruker AXS GmbH, Karlsruhe, Germany) was used to investigate the microstructure of as-prepared Co_2MnSi glass-coated microwires and analyze the phase content (not shown in current work) [42]. The annealed sample showed almost the same XRD profile and apparent structure as reported in our previous work for as-prepared samples [42]. The field cooling and zero-field cooling magnetization curves for temperatures ranging from 5 K to 350 K with an applied external magnetic field of 100 Oe, as well as the room temperature and thermal magnetic behavior of Co_2MnSi glass-coated microwire samples were determined using the Physical Property Magnetic System, PPMS (Quantum Design Inc., San Diego, CA, USA).

3. Results

3.1. Microstructure Analysis

Microstructure analysis was performed using EDX/SEM and XRD to check the chemical composition and structure of the as-prepared and annealed samples. For the chemical composition, the study of the various 10 points yielded the true chemical composition, and the nominal ratio (2:1:1) s accepted since the average chemical composition was about $Co_{51}Mn_{23.9}Si_{25.1}$ for the annealed and as-prepared sample as described in [43]. From the XRD analysis we evaluated the average grain size, D_g, using the Debye–Scherrer equation for sample annealed at 1023 K for 2h and compared the results with the D_g value of the as-prepared sample reported in [43]. The results are provided in Table 1.

Table 1. Average grain size (nm) of annealed and as-prepared Co_2MnSi glass-coated microwire.

| Sample	D_g (nm)
As-prepared	46.2
Annealed at 923 K	50.3
Annealed at 1023 K	64.2

As illustrated in Table 1, the D_g for the samples annealed for 2 h at 923 K and 1023 K was higher than that of the as-prepared sample. For the sample annealed at 923 K (2 h), D_g increased from 46.1 nm to 50.3 nm, i.e., became only 4.2 nm higher than that of the as-prepared sample. For the sample annealed at 1023 K (2 h), a notable increase in D_g of about 18.1 nm was observed, i.e., more than four times higher than the increment observed for the sample annealed at 923 K (2 h) (see Table 1).

As discussed elsewhere, usually the devitrification of amorphous Fe-rich materials by annealing above the crystallization temperature (typically above 823 K) is associated with both increasing grain size and crystalline volume fraction [50]. This kind of tendency in average grain size has also been previously observed in Fe-rich (Finemet-type) glass-coated microwires [51]. However, in microwires with a nanocrystalline structure obtained directly in as-prepared samples, the evolution of the average grain size upon annealing does not always follow this tendency: in some cases (nanocrystalline Fe–Pt microwires), the average grain size did not change considerably upon annealing [52], while even a substantial average grain size refinement has been reported in the case of nanocrystalline Hitperm-like microwires [53]. In discussions of this kind of D_g refinement, proposed mechanisms have included either massive nucleation of small grains upon annealing or even dissolution of the unstable crystalline phases and the nucleation and growth of more stable nanocrystals [53,54]. Additionally, as discussed elsewhere [52], the elevated internal stresses induced during the fabrication process can affect the recrystallization process of materials prepared using rapid melt-quenching methods, due to the nonequilibrium thermodynamics contribution. Indeed, the recrystallization process is substantially affected by atomic diffusion under stress [55]. As mentioned above, the unique feature of the glass-coated microwires is their elevated internal stresses, which can affect the crystallization process of such microwires [43,52,54]. In the present case, the behavior of D_g looks similar to the case of $Fe_{64.7}Pt_{33.3}B_2$ glass-coated microwires, where only a slight annealing effect

on the D_g value was observed for certain annealing temperature ranges. A slight increase observed in D_g is responsible for a minor change in the magnetic properties of the sample annealed at 923 K (2 h) and for a significant change at 1023 K (2 h) as compared to the as-prepared sample, as will be illustrated in the magnetic characterization section.

3.2. Room Temperature Magnetic Properties

To test the magnetic anisotropy at room temperature, the magnetic hysteresis (M-H) loops of Co_2MnSi glass-coated microwire (as-prepared and annealed) were measured at room temperature for two distinct applied external magnetic field directions. First, we measured M-H loops when H was parallel to the axis of the Co_2MnSi glass-coated microwire (i.e., in-plane, IP) and perpendicular to it in the second case (i.e., at an angle of 90 degrees, or out-of-plane, OOP). As can be appreciated from Figure 1a,b, both samples show M-H curves with saturation typical for ferromagnetic behavior and consistent with a Curie point previously reported for these alloys to be well above room temperature (T_c = 985 K) [17]. All hysteresis loops were normalized to the maximum magnetic moment for convenience in comparison. According to Figure 1a,b, both as-prepared and annealed Co_2MnSi glass-coated microwires exhibit strong uniaxial magnetic anisotropy, as evidenced by the considerable difference between the axial and out-of-axis hysteresis loops. Both samples have considerable remanent magnetization in axial hysteresis loops, compared to the out-of-axis hysteresis loop, which exhibits a linear magnetic behavior and a remanence magnetization that is close to zero. As a result, the hard direction of magnetization is perpendicular to the microwire axis, while the easy direction is parallel to it. Magnetic anisotropy is evidenced by the behavior of the axial and out-of-axis hysteresis loops. The annealed sample shows higher values for all magnetic parameters that can be extracted from the M-H loops. The coercivity, H_c, reduced remanence, M_r, and the anisotropy field, H_k, for both directions (IP and the OOP) are summarized in the Table 2. The main point is that the annealed sample presents different magnetic performance compared to the as-prepared sample and that annealing affects the magnetic microstructure of Co_2MnSi microwires and the internal stresses induced during the fabrication process. However, it seems that the annealing conditions do not have a strong impact on the magnetic behavior of the as-prepared sample, since overall magnetic behavior has a similar feature.
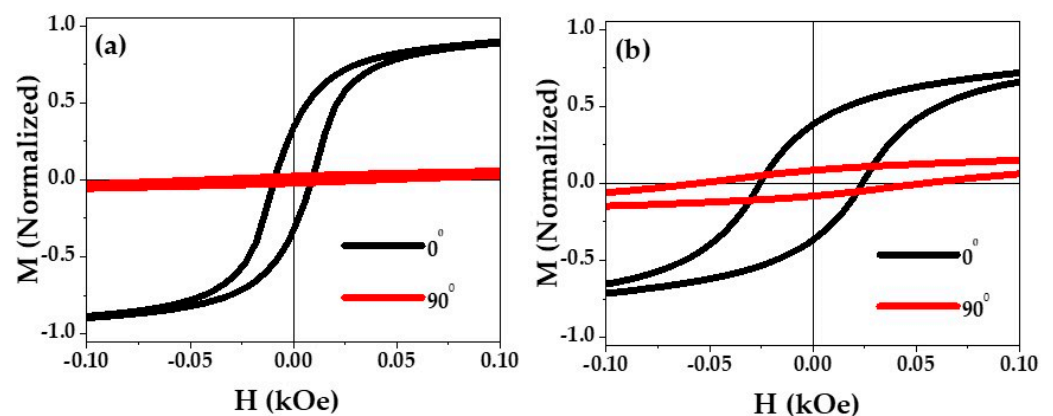
Figure 1. Co_2MnSi glass-coated microwires, both as-prepared samples (**a**) and samples annealed at 1023 K for (2 h) (**b**); in-plane (parallel to the wire axis, black loop) and out-of-plane (perpendicular to the wire axis, red loop) hysteresis loops were measured at room temperature.

Due to the presence of crystalline phases and the former magnetic anisotropy of the microwire, there are two primary sources of this high magnetic anisotropy: cubic magnetocrystalline anisotropy and uniaxial magnetic anisotropy, respectively [47,49,56]. The axial hysteresis loop does not have a precise squared form, as stated for the anisotropic materials, as illustrated in Figure 1. The presence of the amorphous and crystalline phases (see [43]) in our situation is what causes the imperfect squared hysteresis loop. Notably, the

same finding was recently noted in our earlier work using glass-coated microwires with a Co_2-based Heusler alloy [32]. Additionally, our findings coincide with findings for thin films made of Co_2-based Heusler alloys found elsewhere [38].

Table 2. The magnetic parameters of Co_2MnSi glass-coated microwires of as-prepared and annealed samples in IP and OOP directions.

| Samples	H_c (Oe)		M_r		H_k (Oe)	
	IP	OOP	IP	OOP	IP	OOP
As-prepared	9 ± 2	43 ± 2	0.27 ± 0.01	0.02 ± 0.01	440 ± 5	7655 ± 4
Annealed	24 ± 2	56 ± 3	0.15 ± 0.01	0.08 ± 0.01	3200 ± 3	9720 ± 3

3.3. Temperature Dependence of Magnetic Behavior

3.3.1. Zero Field Cooling, Field Cooling, and Field Heating Magnetic Properties

It is critical to examine the entire magnetic behavior of the Co_2MnSi glass-coated microwire at various temperatures in order to assess its thermal stability, a crucial physical characteristic that will help to evaluate its potential interest for spintronics applications. Temperature dependence can also be a valuable indicator of whether a magnetic phase transition is even a possibility. Using a low magnetic field (H = 100 Oe) and a temperature, T, range of 5 to 350 K, we investigated the magnetization dependence on temperature (M vs. T), i.e., zero field cooling (ZFC), field cooling (FC), and field heating (FH) protocols for the as-prepared and annealed Co_2MnSi glass-coated microwires, as shown in Figure 2.

The as-prepared and annealed Co_2MnSi glass-coated microwire samples were cooled to 5 K under an applied magnetic field (H = 100 Oe), causing the random magnetic moment vectors to freeze parallel to the applied field at low temperatures. For the as-prepared sample, almost perfect matching between the ZFC, FC, and FH was observed (see Figure 2a). The interesting point is that all magnetization curves of the as-prepared sample exhibit large, irreversible magnetic behavior where the change in the magnetic tendency occurs at the blocking temperature (200 K). The same magnetization behavior of ZFC, FC, and FH have been observed for annealed samples at 923 K (2h) (see Figure 2b). There is only a slight mismatch between the ZFC, FC, and FH magnetization curves above and below the blocking temperature. In addition, the ZFC and FH magnetization curves overlap the FC curve at a temperature range 50 K–350 K. This difference must be attributed to the changing microstructure of the Co_2MnSi glass-coated microwire during annealing. For the annealed sample at 1023 K (2 h), the ZFC, FC, and FH magnetization curves exhibit complex magnetic behavior compared to the as-prepared sample. As shown in Figure 2c ZFC, FC, and FH magnetization curves exhibit a mismatch. For the ZFC magnetization curve, normalized magnetization starts to decrease with decreasing temperature T within a range of 350 K to 280 K; it then starts increasing with decreasing temperature, reaching a maximum value at T = 210 K. A sharp decrease in normalized magnetization has been observed with decreasing temperature, whereby a minimum value was detected at T = 5 K. This sharp decrease in normalized magnetization indicates large, irreversible magnetic behavior at a blocking temperature of around 210 K. Above this blocking temperature, the FC and FH curves show a different magnetic tendency when the temperature lies within a range of 350 K to 250 K. At this point, the FC and FH have the same tendency when T decreases below 250 K. These differences in the magnetic behavior of the ZFC, FC, and FH are strongly related to the change in the microstructure of the samples with changing the temperature. Such magnetic irreversibility has been shown in Co_2-based Heusler alloy glass-coated microwires [32,36–38]. This irreversibility is highly influenced by the micromagnetic structure of the magnetic materials. Additionally, it appears to be the result of the coexistence of conventional re-entrant ferromagnetism and spin glass-type activity, as previously observed [38,56]. Furthermore, the disordered structure (B2 phase) and chemical makeup of Co_2MnSi glass-coated microwires affect the irreversibility behavior, causing the magnetic ground state to have a strong antiferromagnetic contribution, particularly at low

temperatures for Mn–Mn interaction and random spin disorder (B2 phase), which is also found with the ferromagnetic order (L2$_1$ phase) [17,56].
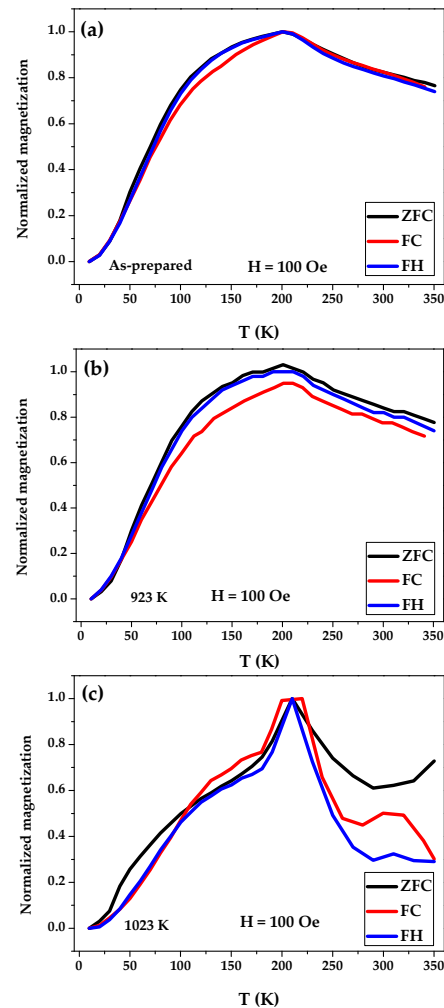

Figure 2. Zero field cooling (ZFC), field cooling (FC) and field heating (FH) of Co$_2$MnSi glass-coated microwires, both as-prepared samples (**a**) and samples annealed at 923 K (2 h) and 1023 K (2 h) (**b**) and (**c**), respectively.

3.3.2. M-H Loops

At this section we focused on the M-H behavior for the as-prepared sample and sample annealed at 1023 K (2 h), where a notable difference in the magnetization curves has been observed as illustrated at Figure 2. The magnetic hysteresis behavior of as-prepared and annealed Co$_2$MnSi glass-coated microwires across a wide range of temperatures (400 K to 5 K) is summarized in Figures 3 and 4. All the M-H loops are represented as M/M$_{5K}$ for a better comparison of the magnetic behavior of the samples, where M$_{5K}$ is the maximum magnetic moment obtained at 5K. The normalized M/M$_{5K}$–values are obtained by normalizing the maximum magnetic moment at different T values to the M$_{5K}$ value. As shown in Figures 3 and 4, all samples, i.e., annealed and as-prepared, exhibit ferromagnetic behavior due to the fact that the Curie point is much higher than room temperature. In addition, the annealed samples exhibit lower normalized saturation magnetization as compared to as-prepared samples. This change must be attributed to a change in the micromagnetic structure as well as to the mechanical stress modification that can be induced by annealing. Moreover, as-prepared Co$_2$MnSi glass-coated microwires yield regular M-H curves with saturation for temperatures ranging between 400 K and 5 K as illustrated in Figures 3 and 4. Meanwhile, the annealed sample does not show a saturation state even for

an applied magnetic field of 30 kOe at temperatures below 50 K. As shown in Figure 4, the slope of the M-H curves increases with decreasing temperature, reaching a maximum at 5 K (see Figure 4d). The unusual magnetic behavior for the annealed sample below 50 K must be attributed to the effect of annealing on the changing microstructure of the Co_2MnSi glass-coated microwire. One of the reasons for the different M-H character of the annealed sample can be enhancement of the antiferromagnetic coupling for Mn-Mn interaction at low temperatures.
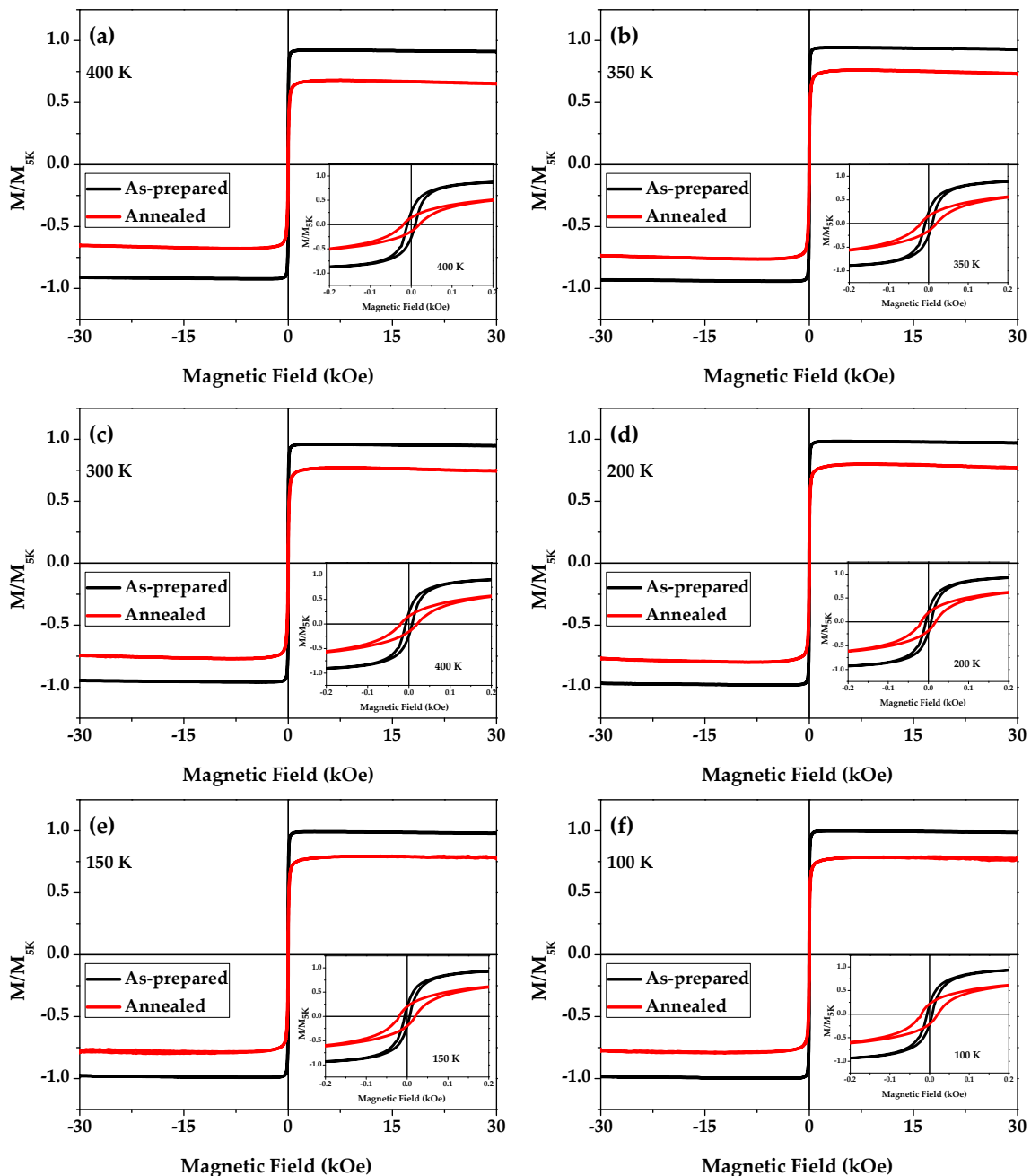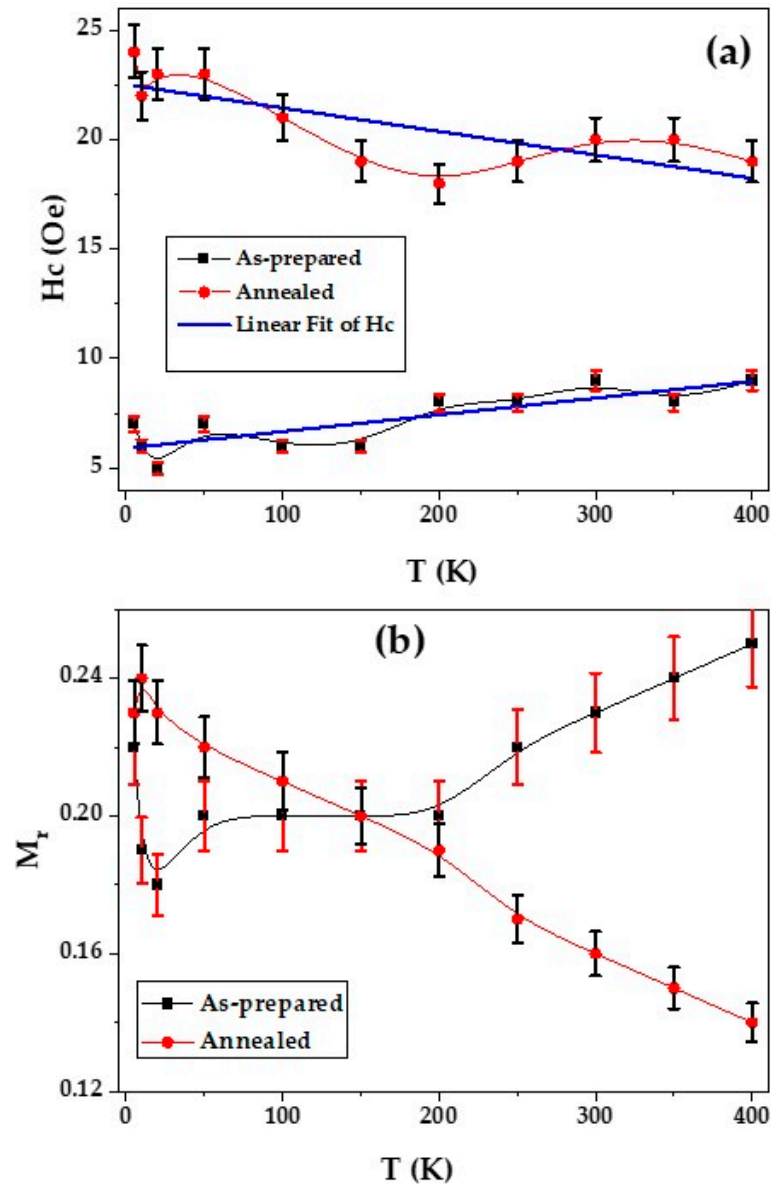

Figure 3. Co_2MnSi glass-coated microwire magnetization curves (M/M_{5K}) for as-prepared samples (black loops) and samples annealed at 1023 K for 2 h (red loops) were measured under a maximum field of 30 kOe and at different temperatures (from 400 K to 100 K). The inset indicates the loops with low scale of the applied magnetic field.
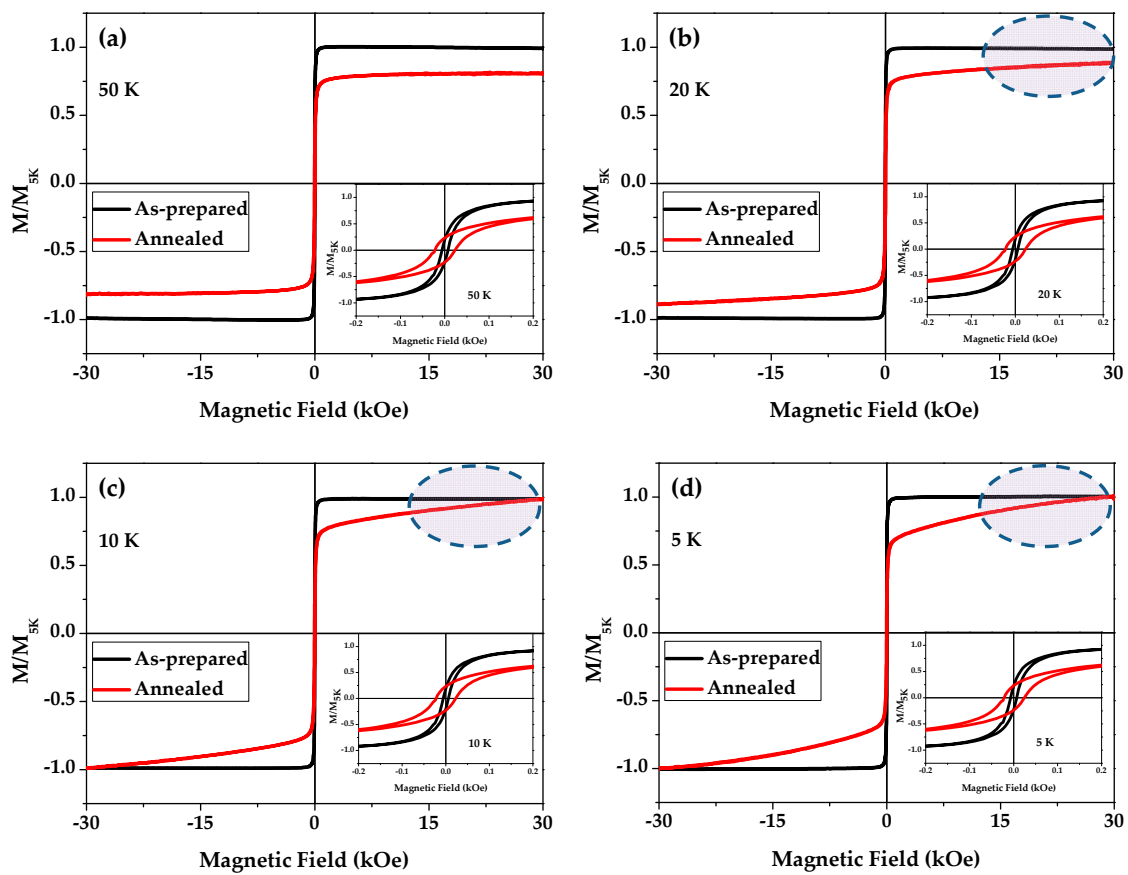
Figure 4. Co_2MnSi glass-coated microwire magnetization curves (M/M_{5K}) for as-prepared samples (black loops) and samples annealed at 1023 K for 2 h (red loops) measured under a maximum field of 30 kOe and at different temperatures (from 50 K to 5 K). The inset indicates the loops with low scale of the applied magnetic field.

From the M-H curves measured at various temperatures in the 5–400 K range, both of as-prepared and annealed Co_2MnSi glass-coated microwires, we can deduce that temperature dependence of H_c and the normalized values of remanence, M_r, exhibit remarkable magnetic behavior. As seen in Figure 5a, coercivity of the annealed sample at 1023 K for 2 h is four times higher than that of the as-prepared sample at all measuring temperature ranges. The interesting aspect of H_c behavior is the small change in H_c with changing T, whereby a difference of around 4 Oe and 6 Oe for the as-prepared and annealed samples, respectively, is observed. Higher coercivity values of the annealed sample can be related to various reasons, such as the different microstructure of the annealed sample, the aforementioned coexistence of ferromagnetic and antiferromagnetic interactions, or even inhomogeneous stress distribution related to the recrystallization process of annealed samples, which can affect the magnetic response to temperature and magnetic field as well. The small variation in coercivity with temperature may manifest the unique thermal stability of coercivity with temperature. This type of H_c stability with temperature can be suitable for various applications. Concerning the M_r temperature dependence, both Co_2MnSi glass-coated microwire samples yield low values, whereby a maximum value of around 0.24 was detected for the sample annealed at 5 K. The low M_r values indicate that the axial magnetization is not dominant, and additional preferred magnetization direction is assumed. Unfortunately, we are not presently able to define the easy magnetization axis of our samples. As illustrated in Figure 5b, M_r behavior as a function of T for the annealed and as-prepared samples is quite unexpected compared to the behavior of H_c. For the temperature range of 400–150 K, the as-prepared and annealed samples exhibit the opposite tendency in $M_r(T)$ dependencies. The behavior then completely changes when T

is below 150 K. This change in $M_r(T)$ tendency must be related to the different processes, such as changes in the internal stresses of the microwires under temperature variation, changes in magnetic ordering, or the different microstructures of as-prepared and annealed samples. The degree to which these variations have an effect is different for the as-prepared and annealed samples, resulting in anomalous magnetic behavior as a function of T as illustrated in Figure 5b.

Figure 5. Coercivity (H_c) of Co_2MnSi glass-coated microwires (the linear fitting of Hc is shown by blue lines.) (**a**) and normalized remanence (M_r) (**b**) dependence on temperature both in as-prepared samples and in samples annealed at 1023 K for 2 h.

As described above, the main peculiar behavior of glass-coated microwires in the presence of the internal stresses is related to the peculiarities of the fabrication process [43,46,57,58]. The main origin of such internal stresses is related to the different thermal expansion coefficients of the metallic nuclei and glass-coating [3,43,46,57,58]. However, the magnetoelastic anisotropy related to these internal stresses can be partially released by annealing, while further crystallization of the amorphous phase (either average growth in grain size or crystalline phase content) or phase transformation induced by annealing can also affect the magnetic behavior of glass-coated microwires. In the present study we focus only on the effect of an-

nealing on the magnetic properties. Further studies can help to understand higher coercivity of the annealed sample.

4. Conclusions

In summary, in the current study we focus on the effect of the annealing temperature on the magnetic properties of Co_2MnSi glass-coated microwires. A significant change in the magnetic properties was observed in samples annealed at 1023 K (2 h) compared to as-prepared samples; minor changes were observed in the magnetic properties of samples annealed at 923 K (2 h) due to slight changes in its microstructure, as illustrated in the structure investigation section of this study. Below this annealing temperature, the magneto-structural behavior did not show any significant change, which verifies the unique thermal stability of Co_2MnSi glass-coated microwires as a function of temperature. An increase in the coercivity value was observed for the annealed sample compared to the as-prepared sample. A shift in the blocking temperature of annealed samples toward room temperature from 200 K to 210 K was detected. Both annealed and as-prepared Co_2MnSi glass-coated microwires exhibited relatively low normalized remanence, which indicates that the easy magnetization axis does not exist perfectly parallel to the microwire axis. Thus, further structure and angular magnetic investigations are necessary in order to illustrate the effects of annealing conditions on the behavior of the microwires studied. For the application possibilities, the quiet thermal stability of the soft coercivity values of annealed and as-prepared Co_2MnSi glass-coated microwires can be integrated in generators, transformers, and switching circuits based on glass-coated microwires.

Author Contributions: Conceptualization, M.S. and A.Z.; methodology, V.Z. and P.C.-L.; validation, M.S., V.Z. and A.Z.; formal analysis, M.S. and A.Z.; investigation, M.S., A.Z., V.Z. and P.C.-L.; resources, V.Z. and A.Z.; data curation, M.I. and A.Z.; writing—original draft preparation, M.S. and A.Z.; writing—review and editing, M.S. and A.Z.; visualization, M.S., M.I. and A.Z.; supervision, A.Z.; project administration, V.Z. and A.Z.; funding acquisition, V.Z. and A.Z. All authors have read and agreed to the published version of the manuscript.

Data Availability Statement: Not applicable.

Conflicts of Interest: The authors declare no conflict of interest.

References

1. Taylor, G.F. A Method of Drawing Metallic Filaments and a Discussion of Their Properties and Uses. *Phys. Rev.* **1924**, *23*, 655. [CrossRef]
2. Ulitovsky, A.V.; Maianski, I.M. Avramenco A I 1960 Method of Continuous Casting of Glass Coated Microwire. USSR Patent 128427, 15 May 1960.
3. Zhukov, A.; Corte-Leon, P.; Gonzalez-Legarreta, L.; Ipatov, M.; Blanco, J.M.; Gonzalez, A.; Zhukova, V. Advanced Functional Magnetic Microwires for Technological Applications. *J. Phys. D Appl. Phys.* **2022**, *55*, 253003. [CrossRef]
4. Jurc, R.; Frolova, L.; Kozejova, D.; Fecova, L.; Hennel, M.; Galdun, L.; Richter, K.; Gamcova, J.; Ibarra, P.; Hudak, R.; et al. *Sensoric Application of Glass-Coated Magnetic Microwires*, 2nd ed.; Elsevier Ltd.: Amsterdam, The Netherlands, 2020; ISBN 9780081028322.
5. Zhukova, V.; Corte-Leon, P.; Blanco, J.M.; Ipatov, M.; Gonzalez-Legarreta, L.; Gonzalez, A.; Zhukov, A. Development of Magnetically Soft Amorphous Microwires for Technological Applications. *Chemosensors* **2022**, *10*, 26. [CrossRef]

6. Baranov, S.A.; Larin, V.S.; Torcunov, A.V. Technology, Preparation and Properties of the Cast Glass-Coated Magnetic Microwires. *Crystals* **2017**, *7*, 136. [CrossRef]

7. Inomata, K.; Ikeda, N.; Tezuka, N.; Goto, R.; Sugimoto, S.; Wojcik, M.; Jedryka, E. Highly Spin-Polarized Materials and Devices for Spintronics. *Adv. Mater.* **2008**, *9*, 14101. [CrossRef]

8. Chumak, O.M.; Pacewicz, A.; Lynnyk, A.; Salski, B.; Yamamoto, T.; Seki, T.; Domagala, J.Z.; Głowiński, H.; Takanashi, K.; Baczewski, L.T.; et al. Magnetoelastic Interactions and Magnetic Damping in $Co_2Fe_{0.4}Mn_{0.6}Si$ and $Co_2FeGa_{0.5}Ge_{0.5}$ Heusler Alloys Thin Films for Spintronic Applications. *Sci. Rep.* **2021**, *11*, 7608. [CrossRef]

9. De Groot, R.A.; Mueller, F.M.; Engen, P.G.V.; Buschow, K.H.J. New Class of Materials: Half-Metallic Ferromagnets. *Phys. Rev. Lett.* **1983**, *50*, 2024. [CrossRef]

10. Elphick, K.; Frost, W.; Samiepour, M.; Kubota, T.; Takanashi, K.; Sukegawa, H.; Mitani, S.; Hirohata, A. Heusler Alloys for Spintronic Devices: Review on Recent Development and Future Perspectives. *Sci. Technol. Adv. Mater.* **2021**, *22*, 235–271. [CrossRef]

11. Bai, Z.; Shen, L.E.I.; Han, G.; Feng, Y.P. Data Storage: Review of Heusler Compounds. *Spin* **2012**, *2*, 1230006. [CrossRef]

12. Galanakis, I.; Dederichs, P.H.; Papanikolaou, N. Slater-Pauling Behavior and Origin of the Half-Metallicity of the Full-Heusler Alloys. *Phys. Rev. B* **2002**, *66*, 174429. [CrossRef]

13. Hazra, B.K.; Kaul, S.N.; Srinath, S.; Raja, M.M. Uniaxial Anisotropy, Intrinsic and Extrinsic Damping in Co_2FeSi Heusler Alloy Thin Films. *J. Phys. D Appl. Phys.* **2019**, *52*, 325002. [CrossRef]

14. Wurmehl, S.; Fecher, G.H.; Kandpal, H.C.; Ksenofontov, V.; Felser, C.; Lin, H.J.; Morais, J. Geometric, Electronic, and Magnetic Structure of Co_2FeSi: Curie Temperature and Magnetic Moment Measurements and Calculations. *Phys. Rev. B Condens. Matter. Mater. Phys* **2005**, *72*, 184434. [CrossRef]

15. Li, P.; Koo, J.; Ning, W.; Li, J.; Miao, L.; Min, L.; Zhu, Y.; Wang, Y.; Alem, N.; Liu, C.X.; et al. Giant Room Temperature Anomalous Hall Effect and Tunable Topology in a Ferromagnetic Topological Semimetal Co_2MnAl. *Nat. Commun.* **2020**, *11*, 3476. [CrossRef]

16. Belopolski, I.; Manna, K.; Sanchez, D.S.; Chang, G.; Ernst, B.; Yin, J.; Zhang, S.S.; Cochran, T.; Shumiya, N.; Zheng, H.; et al. Discovery of Topological Weyl Fermion Lines and Drumhead Surface States in a Room Temperature Magnet. *Science* **2019**, *365*, 1278–1281. [CrossRef]

17. Ahmed, S.J.; Boyer, C.; Niewczas, M. Magnetic and Structural Properties of Co_2MnSi Based Heusler Compound. *J. Alloys Compd.* **2019**, *781*, 216–225. [CrossRef]

18. Guillemard, C.; Petit-Watelot, S.; Pasquier, L.; Pierre, D.; Ghanbaja, J.; Rojas-Sánchez, J.C.; Bataille, A.; Rault, J.; le Fèvre, P.; Bertran, F.; et al. Ultralow Magnetic Damping in Co_2Mn -Based Heusler Compounds: Promising Materials for Spintronics. *Phys. Rev. Appl.* **2019**, *11*, 064009. [CrossRef]

19. Liu, H.X.; Honda, Y.; Taira, T.; Matsuda, K.I.; Arita, M.; Uemura, T.; Yamamoto, M. Giant Tunneling Magnetoresistance in Epitaxial $Co_2MnSi/MgO/Co_2MnSi$ Magnetic Tunnel Junctions by Half-Metallicity of Co_2MnSi and Coherent Tunneling. *Appl. Phys. Lett.* **2012**, *101*, 132418. [CrossRef]

20. Stuelke, L.; Kharel, P.; Shand, P.M.; Lukashev, P.V. First Principles Study of Perpendicular Magnetic Anisotropy in Thin-Film Co_2MnSi. *Phys. Scr.* **2021**, *96*, 125818. [CrossRef]

21. Ishida, S.; Fujii, S.; Kashiwagi, S.; Asano, S. Search for Half-Metallic Compounds in Co_2MnZ (Z=IIIb, IVb, Vb Element). *J. Phys. Soc. Jpn.* **1995**, *64*, 2152–2157. [CrossRef]

22. Pradines, B.; Arras, R.; Abdallah, I.; Biziere, N.; Calmels, L. First-Principles Calculation of the Effects of Partial Alloy Disorder on the Static and Dynamic Magnetic Properties of Co_2MnSi. *Phys. Rev. B* **2017**, *95*, 094425. [CrossRef]

23. Cheng, S.F.; Nadgorny, B.; Bussmann, K.; Carpenter, E.E.; Das, B.N.; Trotter, G.; Raphael, M.P.; Harris, V.G. Growth and Magnetic Properties of Single Crystal Co_2MnX (X = Si, Ge) Heusler Alloys. *IEEE Trans. Magn.* **2001**, *37*, 2176–2178. [CrossRef]

24. Jourdan, M.; Minár, J.; Braun, J.; Kronenberg, A.; Chadov, S.; Balke, B.; Gloskovskii, A.; Kolbe, M.; Elmers, H.J.; Schönhense, G.; et al. Direct Observation of Half-Metallicity in the Heusler Compound Co_2MnSi. *Nat. Commun.* **2014**, *5*, 3974. [CrossRef]

25. Wang, B.; Liu, Y. Exchange Bias and Inverse Magnetocaloric Effect in Co and Mn Co-Doped Ni_2MnGa Shape Memory Alloy. *Metals* **2013**, *3*, 69–76. [CrossRef]

26. Dunand, D.C.; Müllner, P. Size Effects on Magnetic Actuation in Ni-Mn-Ga Shape-Memory Alloys. *Adv. Mater.* **2011**, *23*, 216–232. [CrossRef]

27. Felser, C.; Hirohata, A. (Eds.) *Heusler Alloys*; Springer Series in Materials Science; Springer International Publishing: Cham, Switzerland, 2016; Volume 222, ISBN 978-3-319-21448-1.

28. Salaheldeen, M.; Nafady, A.; Abu-Dief, A.M.; Díaz Crespo, R.; Fernández-García, M.P.; Andrés, J.P.; López Antón, R.; Blanco, J.A.; Álvarez-Alonso, P. Enhancement of Exchange Bias and Perpendicular Magnetic Anisotropy in CoO/Co Multilayer Thin Films by Tuning the Alumina Template Nanohole Size. *Nanomaterials* **2022**, *12*, 2544. [CrossRef]

29. Salaheldeen, M.; Abu-Dief, A.M.; Martínez-Goyeneche, L.; Alzahrani, S.O.; Alkhatib, F.; Álvarez-Alonso, P.; Blanco, J.Á. Dependence of the Magnetization Process on the Thickness of $Fe_{70}Pd_{30}$ Nanostructured Thin Film. *Materials* **2020**, *13*, 5788. [CrossRef]

30. Zhukov, A.; Rodionova, V.; Ilyn, M.; Aliev, A.M.; Varga, R.; Michalik, S.; Aronin, A.; Abrosimova, G.; Kiselev, A.; Ipatov, M.; et al. Magnetic Properties and Magnetocaloric Effect in Heusler-Type Glass-Coated NiMnGa Microwires. *J. Alloys Compd.* **2013**, *575*, 73–79. [CrossRef]

31. Salaheldeen, M.; Vega, V.; Caballero-Flores, R.; Prida, V.M.; Fernández, A. Influence of nanoholes array geometrical parameters on magnetic properties of Dy–Fe antidot thin films. *Nanotechnology* **2019**, *30*, 455703. [CrossRef]

32. Chiriac, H.; Lupu, N.; Stoian, G.; Ababei, G.; Corodeanu, S.; Óvári, T.-A. Ultrathin Nanocrystalline Magnetic Wires. *Crystals* **2017**, *7*, 48. [CrossRef]

33. Salaheldeen, M.; Garcia-Gomez, A.; Ipatov, M.; Corte-Leon, P.; Zhukova, V.; Blanco, J.M.; Zhukov, A. Fabrication and Magneto-Structural Properties of Co2-Based Heusler Alloy Glass-Coated Microwires with High Curie Temperature. *Chemosensors* **2022**, *10*, 225. [CrossRef]

34. Salaheldeen, M.; Ipatov, M.; Zhukova, V.; García-Gomez, A.; Gonzalez, J.; Zhukov, A. Preparation and magnetic properties of Co2-based Heusler alloy glass-coated microwires with high Curie temperature. *AIP Adv.* **2023**, *13*, 025325. [CrossRef]

35. Zhukova, V.; Corte-Leon, P.; González-Legarreta, L.; Talaat, A.; Blanco, J.M.; Ipatov, M.; Olivera, J.; Zhukov, A. Review of Domain Wall Dynamics Engineering in Magnetic Microwires. *Nanomaterials* **2020**, *10*, 2407. [CrossRef]

36. Salaheldeen, M.; Garcia-Gomez, A.; Corte-Leon, P.; Ipatov, M.; Zhukova, V.; Gonzalez, J.; Zhukov, A. Anomalous Magnetic Behavior in Half-Metallic Heusler Co_2FeSi Alloy Glass-Coated Microwires with High Curie Temperature. *J. Alloys Compd.* **2022**, *923*, 166379. [CrossRef]

37. Salaheldeen, M.; Garcia-Gomez, A.; Corte-León, P.; Gonzalez, A.; Ipatov, M.; Zhukova, V.; Gonzalez, J.M.; López Antón, R.; Zhukov, A. Manipulation of Magnetic and Structure Properties of Ni_2FeSi Glass-Coated Microwires by Annealing. *J. Alloys Compd.* **2023**, *942*, 169026. [CrossRef]

38. Salaheldeen, M.; Garcia, A.; Corte-Leon, P.; Ipatov, M.; Zhukova, V.; Zhukov, A. Unveiling the Effect of Annealing on Magnetic Properties of Nanocrystalline Half-Metallic Heusler Co_2FeSi Alloy Glass-Coated Microwires. *J. Mater. Res. Technol.* **2022**, *20*, 4161–4172. [CrossRef]

39. Mitxelena-Iribarren, O.; Campisi, J.; Martínez de Apellániz, I.; Lizarbe-Sancha, S.; Arana, S.; Zhukova, V.; Mujika, M.; Zhukov, A. Glass-Coated Ferromagnetic Microwire-Induced Magnetic Hyperthermia for in Vitro Cancer Cell Treatment. *Mater. Sci. Eng. C* **2020**, *106*, 110261. [CrossRef] [PubMed]

40. Talaat, A.; Alonso, J.; Zhukova, V.; Garaio, E.; García, J.A.; Srikanth, H.; Phan, M.H.; Zhukov, A. Ferromagnetic Glass-Coated Microwires with Good Heating Properties for Magnetic Hyperthermia. *Sci. Rep.* **2016**, *6*, 39300. [CrossRef] [PubMed]

41. Kozejova, D.; Fecova, L.; Klein, P.; Sabol, R.; Hudak, R.; Sulla, I.; Mudronova, D.; Galik, J.; Varga, R. Biomedical Applications of Glass-Coated Microwires. *J. Magn. Magn. Mater.* **2019**, *470*, 2–5. [CrossRef]

42. Salaheldeen, M.; Talaat, A.; Ipatov, M.; Zhukova, V.; Zhukov, A. Preparation and Magneto-Structural Investigation of Nanocrystalline CoMn-Based Heusler Alloy Glass-Coated Microwires. *Processes* **2022**, *10*, 2248. [CrossRef]

43. Zhukov, A.; Ipatov, M.; Talaat, A.; Blanco, J.M.; Hernando, B.; Gonzalez-Legarreta, L.; Suñol, J.J.; Zhukova, V. Correlation of Crystalline Structure with Magnetic and Transport Properties of Glass-Coated Microwires. *Crystals* **2017**, *7*, 41. [CrossRef]

44. Vázquez, M.; Zhukov, A.; Aragoneses, P.; Arcas, J.; Marin, P.; Hernando, A. Magneto-impedance of glass-coated amorphous CoMnSiB microwires. *IEEE Trans. Magn.* **1998**, *34*, 724–728. [CrossRef]

45. Zhukov, A.; Ipatov, M.; del Val, J.J.; Zhukova, V.; Chernenko, V.A. Magnetic and Structural Properties of Glass-Coated Heusler-Type Microwires Exhibiting Martensitic Transformation. *Sci. Rep.* **2018**, *8*, 621. [CrossRef] [PubMed]

46. Torcunov, A.V.; Baranov, S.A.; Larin, V.S. The Internal Stresses Dependence of the Magnetic Properties of Cast Amorphous Microwires Covered with Glass Insulation. *J. Magn. Magn. Mater.* **1999**, *196–197*, 835–836. [CrossRef]

47. Guo, X.B.; Zuo, Y.L.; Cui, B.S.; Li, D.; Yun, J.J.; Wu, K.; Wang, T.; Xi, L. Post Annealing Induced Magnetic Anisotropy in CoFeSi Thin Films on MgO(0 0 1). *J. Phys. D Appl. Phys.* **2017**, *50*, 085006. [CrossRef]

48. Salaheldeen, M.; Wederni, A.; Ipatov, M.; Gonzalez, J.; Zhukova, V.; Zhukov, A. Elucidation of the Strong Effect of the Annealing and the Magnetic Field on the Magnetic Properties of Ni_2-Based Heusler Microwires. *Crystals* **2022**, *12*, 1755. [CrossRef]

49. Gunnarsson, K.; Svedlindh, P.; Andersson, J.O.; Nordblad, P.; Lundgren, L.; Aruga Katori, H.; Ito, A. Magnetic Behavior of a Reentrant Ising Spin Glass. *Phys. Rev. B* **1992**, *46*, 8227–8231. [CrossRef]

50. Herzer, G. Anisotropies in soft *magnetic* nanocrystalline alloys. *J. Magn. Magn. Mater.* **2005**, *294*, 99–106. [CrossRef]

51. Talaat, A.; Zhukova, V.; Ipatov, M.; del Val, J.J.; Blanco, J.M.; Gonzalez-Legarreta, L.; Hernando, B.; Churyukanova, M.; Zhukov, A. Engineering of Magnetic Softness and Magnetoimpedance in Fe-Rich Microwires by Nanocrystallization. *JOM* **2016**, *68*, 1563–1571. [CrossRef]

52. Zhukova, V.; Talaat, A.; del Val, J.J.; Ipatov, M.; Zhukov, A. Preparation and Characterization of Fe-Pt and Fe-Pt-(B, Si) Microwires. *IEEE Magn. Lett.* **2016**, *7*, 5200704. [CrossRef]

53. Talaat, A.; del Val, J.J.; Zhukova, V.; Ipatov, M.; Klein, P.; Varga, R.; González, J.; Churyukanova, M.; Zhukov, A. Grain size refinement in nanocrystalline Hitperm-type glass-coated microwires. *J. Magn. Magn. Mater.* **2016**, *406*, 15–21. [CrossRef]

54. Serebryakov, A.V. Amorphization reactions and glass to crystal transformations in metallic materials. *J. Non-Cryst. Solids* **1993**, *156–158*, 594–597. [CrossRef]

55. Onsager, L. Reciprocal relations in irreversible processes. I. *Phys. Rev.* **1931**, *37*, 405–426. [CrossRef]

56. Yang, F.; Li, W.; Li, J.; Chen, H.; Liu, D.; Chen, X.; Yang, C. The Microstructure and Magnetic Properties of Co_2MnSi Thin Films Deposited on Si Substrate. *J. Alloys Compd.* **2017**, *723*, 188–191. [CrossRef]

57. Chiriac, H.; Ovari, T.-A. Amorphous glass-covered magnetic wires: Preparation, properties, applications. *Prog. Mater. Sci.* **1996**, *40*, 333–407. [CrossRef]

58. Zhukova, V.; Blanco, J.M.; Ipatov, M.; Zhukov, A. Magnetoelastic contribution in domain wall dynamics of amorphous microwires. *Phys. B Condens. Matter* **2012**, *407*, 1450–1454. [CrossRef]